POLITECNICO DI TORINO
Repository ISTITUZIONALE

Modeling of 3D feeding structures in the automated design of metasurface antennas

(Article begins on next page)

01 May 2024

Modeling of 3D Feeding Structures in the Automated Design of Metasurface Antennas

L. Teodorani*, M. Zucchi*, G. Vecchi*

*Department of Electronics and Telecommunications, Politecnico di Torino, Torino, Italy;

{lucia.teodorani,marcello.zucchi,giuseppe.vecchi}@polito.it

Abstract—We present an automatic procedure to fully design a metasurface antenna, including the feeding structure. This feature is achieved by performing preliminary full-wave simulations of the feeding structure and by properly modelling PEC regions inside a current-based numerical design method. The synthesized metasurface antennas are implemented and simulated with a full-wave commercial solver, showing excellent agreement with the predicted performances.

Index Terms—Impedance boundary condition, integral equations, method of moments, metasurface antennas, optimization.

I. INTRODUCTION

In the design of metasurface antennas, the modelling of the feeding structure is of paramount importance for the correct estimation of the realized gain (and the S_{11}) of the antenna. Moreover, a non-ideal source can be responsible for spurious radiation that affects the overall radiation pattern of the synthesized metasurface antenna.

In [1], an automatic 3D method for the design of metasurface antennas, starting from arbitrary mask-type specifications on the radiated field and realizability constraints on the values of the synthesizable surface reactance, was described. This method involves the optimization of the metasurface equivalent current only, and relies on a computationally-efficient formulation of the optimization instance that allows to compute all functional and gradient evaluations with a limited number of matrix-vector products. The incident field is arbitrary; in particular, the method can handle the case of on-surface excitation, as necessary in low-profile metasurface antennas.

In this paper, we employ the automatic method described in [1] to fully design metasurface antennas by taking into account *real* 3D feeding structures. This feature is achieved by integrating the design process with a preliminary step involving full-wave simulations of the feeding structure carried out with commercial solvers. Moreover, a new term is added to the optimization cost function presented in [1] relative to the minimization of the norm of the electric field on PEC structures. A very preliminary similar approach was described in a previous conference paper [2], that however did not include the modeling of the launching structure inside the optimization instance.

II. DESIGN METHODOLOGY

The detailed description of the adopted numerical procedure for the automated design of metasurfaces is reported in [1]
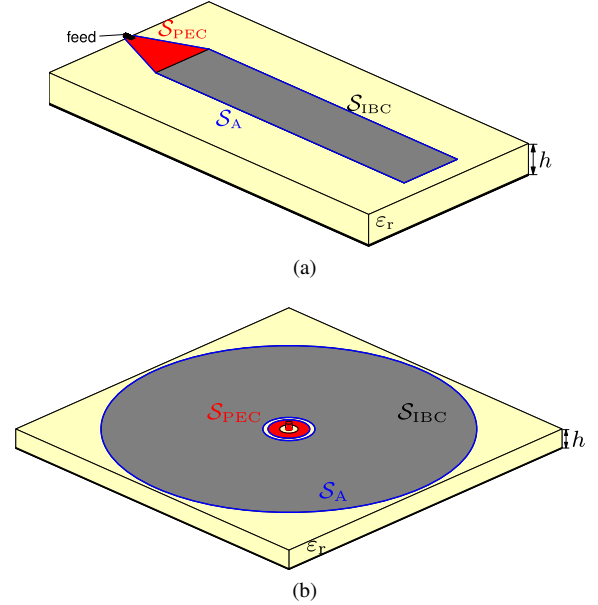

Fig. 1. Examples of the metasurface antennas: (a) rectangular geometry, (b) circular geometry.

and will be omitted here. This method requires as inputs the antenna geometry, the incident field on the metasurface, the constraints on the synthesizable impedance and the desired radiation pattern. While it is possible to define the incident field $\boldsymbol{E}_{\text{inc}}$ in an analytical way, this choice does not accurately represent the field generated by a realistic feed, which typically consists of an electromagnetic source and a beam-forming structure.

In this work, we consider two different launching structures and antenna layouts, as shown in Fig. 1. Here, $\mathcal{S}_{\text{IBC}}$ indicates the unknown impedance region that must be synthesized by the numerical method, $\mathcal{S}_{\text{PEC}}$ represents a PEC region (*known* impedance), while $\mathcal{S}_{\text{A}}$ comprises the whole antenna surface. In the rectangular layout (Fig. 1a), the source of the incident field is on-surface, and the PEC region is introduced to represent the tapered section used to connect the feed to the radiating metasurface. In the circular type (Fig. 1b), a vertical pin is placed at the center of the antenna, and an annular ring provides matching to the surrounding surface; in this case, the feed is represented by the equivalent magnetic currents located at the insertion of the input coaxial cable into the ground plane.

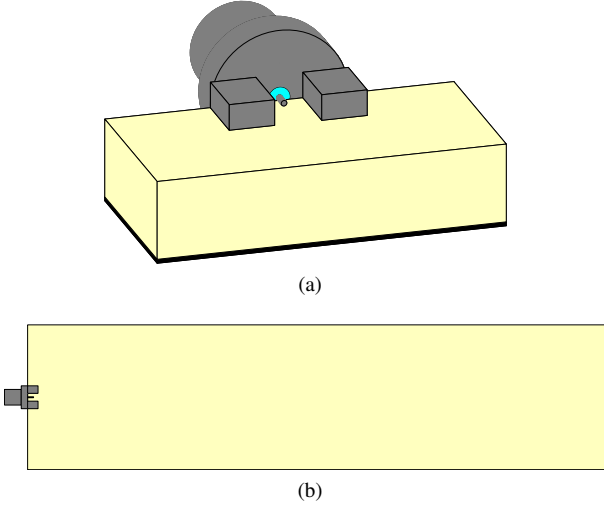The first step of our design process consists in the simulation

(a)

(b)

Fig. 2. Setup for the simulation of the real antenna feed and extraction of the incident electric field using a commercial solver: (a) 3D model of the coaxial feed, (b) top view of the feed placed on the grounded dielectric substrate in absence of metallizations.

of the real antenna feed, without the metasurface, with a full-wave commercial solver, in order to obtain the input $\boldsymbol{E}_{\text{inc}}$ for the automated numerical method. Fig. 2 shows the $50\,\Omega$ coaxial feed used for the rectangular metasurface and the simulation setup in CST Studio Suite [3]. For the circular geometry, the incident field generated by the magnetic currents located on the ground plane is obtained using a in-house solver based on the Method of Moments.

The second step involves the optimization of the launching structure that will connect the feed to the actual radiating metasurface. For the rectangular metasurface, this section is designed, via full-wave optimizations, to match the coaxial feed to the input impedance of a microstrip as wide as the metasurface area; in case of circular metasurface, the central pin's height and the annular ring's dimensions (see Fig. 1b) are optimized to minimize the reflection coefficient and maximize the power flow inside the dielectric substrate.

Finally, these structures will then be accounted for in the automated design process as PEC regions, by imposing that the electric field be null on the cells belonging to $\mathcal{S}_{\text{PEC}}$, i.e.,

$$|\boldsymbol{E}_{\text{tan}}(\boldsymbol{r})|^2 = 0, \qquad \forall \boldsymbol{r} \in \mathcal{S}_{\text{PEC}} \qquad (1)$$

The corresponding functional is added to the cost function of [1].

III. RESULTS

A. Rectangular Metasurface

The rectangular metasurface, that can be interpreted as a leaky-wave antenna, is designed to achieve broadside radiation. This is typically hard to obtain due to the presence of an open stopband that leads to a nearly-total reflection of the traveling wave [4].

The design is carried out at $10\,\text{GHz}$. A $2.286\,\text{mm}$-thick RO3006 substrate ($\varepsilon_r = 6.5$) is used. The optimized current
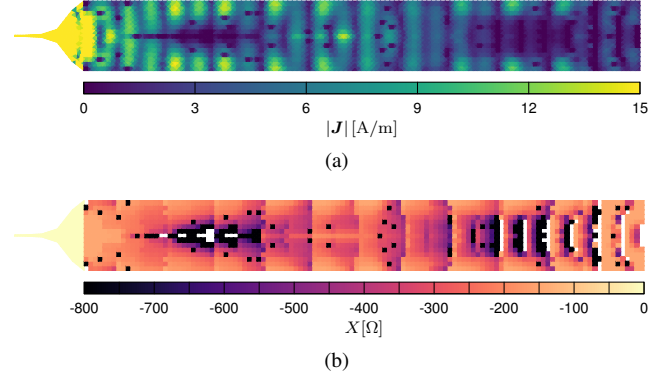

Fig. 3. Design outputs for the RO3006 solution: (a) optimum current density returned as output of the numerical method and (b) the corresponding impedance pattern.

density returned by the automated method and the corresponding impedance pattern are shown in Fig. 3, while the imposed far-field constraints are pictured together with the radiation pattern generated by the synthesized metasurface in Fig. 4. There is excellent agreement between the far-field pattern returned by the automated method and the one obtained with full-wave simulations of the designed antenna in the commercial solver; the unconventional impedance pattern effectively eliminates the open stopband problem, and the correct modelling of the input field and the launching structure, according to the proposed technique, proves fundamental for ensuring broadside radiation is achieved with a physically-realizable prototype.
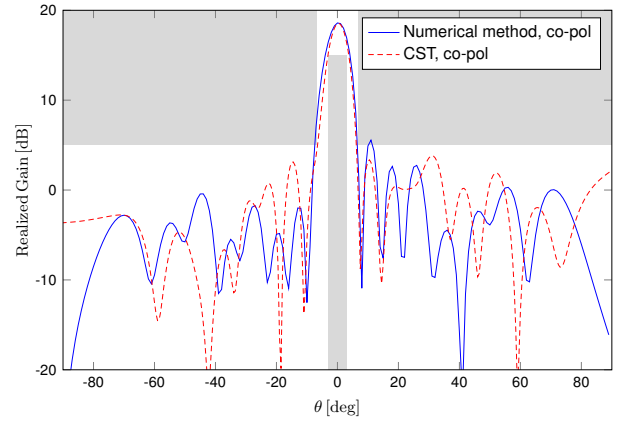

Fig. 4. Comparison of far-field pattern obtained from the numerical method and the one produced by CST simulation of the antenna for the rectangular geometry.

B. Circular Metasurface

The circular antenna is designed to generate a pencil beam with circular polarization. The design frequency is $23\,\text{GHz}$ and a dielectric substrate of thickness $1.27\,\text{mm}$ and $\varepsilon_r = 3$ is used. The optimized current density returned by the automated method and the corresponding impedance pattern are shown in Fig. 5, while the radiation pattern generated by the synthesized
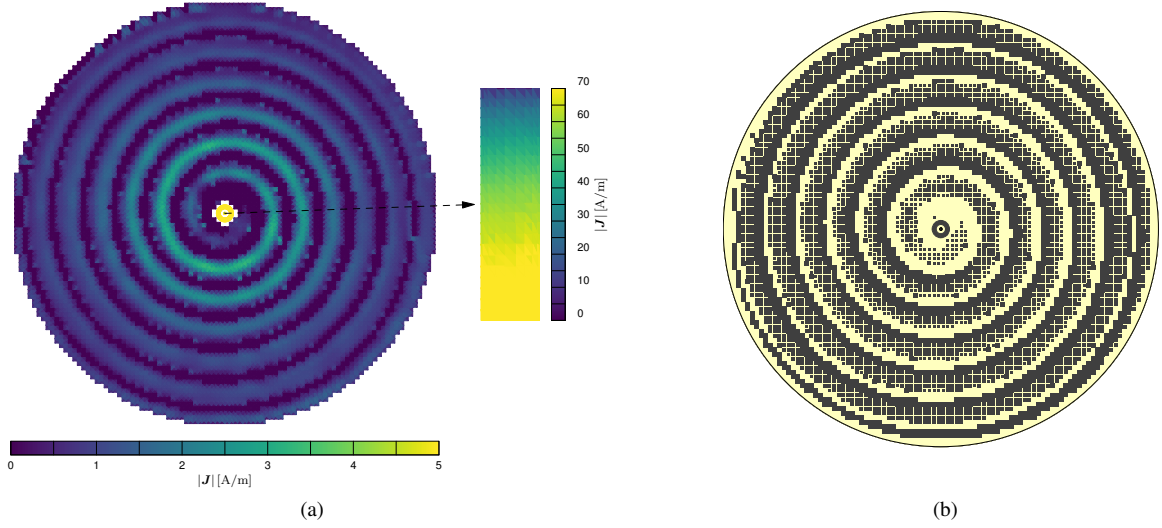
Fig. 5. Design outputs for the circular solution: (a) optimum current density and (b) implementation via square patches of the synthesized impedance. The inset in (a) shows the current on the central pin.

metasurface is pictured in Fig. 6. The impedance profile obtained with the proposed numerical method follows a spiral shape. There is very good agreement between the expected far-field pattern and the simulated one; the difference in the sidelobe level is due to the fact that the numerical method considers an infinite dielectric substrate for the computation of the multilayer Green's function, while the substrate in the full-wave simulation is limited. In fact, "open" boundary conditions (with extra space for far-field calculation) were set in the CST simulation environment, in order to estimate the radiation pattern that would be generated by *actual* physical prototypes of the designed antennas.
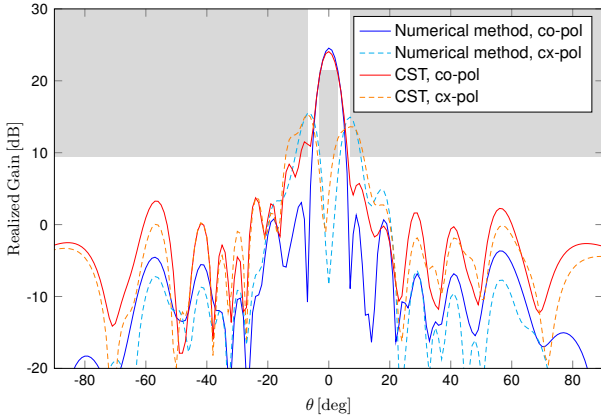

Fig. 6. Comparison of far-field pattern obtained from the numerical method and the one produced by CST simulation of the antenna for the circular geometry.

IV. CONCLUSION

We have presented a design methodology for the automated design of metasurface antennas that fully includes realistic feeding structures in the synthesis process. This feature is achieved by performing preliminary full-wave simulations that allow to extract the correct input incident field for a current-based numerical method and by modelling the launching structures as PEC regions. The proposed technique is applied to the design of two different metasurface geometries, proving its validity in the accurate prediction of the synthesized antennas' performances.

REFERENCES

[1] M. Zucchi, F. Vernì, M. Righero, and G. Vecchi, "Current Based Automated Design of Realizable Metasurface Antennas With Arbitrary Pattern Constraints," *IEEE Trans. Antennas Propag.*, vol. 71, no. 6, pp. 4888–4902, Jun. 2023.
[2] L. Teodorani, M. Zucchi, and G. Vecchi, "Numerically-Synthesized Broadside-Radiating Leaky-Wave Antenna," in *2023 IEEE Int. Symp. Antennas Propag. USNC-URSI Radio Sci. Meet. AP-SURSI*, Jul. 2023, pp. 1–2.
[3] Dassault Systèmes Simulia, "CST Studio Suite 2022," www.cst.com.
[4] D. R. Jackson, C. Caloz, and T. Itoh, "Leaky-Wave Antennas," *Proc. IEEE*, vol. 100, no. 7, pp. 2194–2206, Jul. 2012.